Spring 5-2022

Optophysiology of D. Melanogaster Neuromuscular Synapses Using GCaMP

Kavindra Dasrat

Optophysiology of *D. Melanogaster* Neuromuscular Synapses Using GCaMP

An honors thesis presented to the
Department of Biological Sciences,
University at Albany, State University of New York
in partial fulfillment of the requirements
for graduation with Honors in Biology
and
graduation from the Honors College

Kavindra Dasrat

Research Advisor: Gregory Lnenicka, Ph.D.
Second Reader: Damian G. Zuloaga, Ph.D.

May 2022

Abstract

An activity-dependent increase in postsynaptic currents produced by a single vesicle of neurotransmitter is an important mechanism for synaptic plasticity in the central nervous system (CNS) and possibly involved in learning and memory. We have found a similar form of postsynaptic potentiation at the *D. Melanogaster* neuromuscular junction (NMJ) where a brief increase in impulse activity results in an increase in the amplitude of spontaneous miniature excitatory postsynaptic currents (mEPSCs), resulting in miniature excitatory postsynaptic potentials (mEPSPs). To visualize sites of postsynaptic potentiation along the synaptic terminal, we have used a Ca^{2+} indicator, GCaMP to observe postsynaptic Ca^{2+} signals. Since the postsynaptic glutamate receptors admit Ca^{2+}, these postsynaptic Ca^{2+} signals should reflect the magnitude of the mEPSCs. We can observe the postsynaptic potentiation using this technique since a brief increase in impulse activity produces an increase in the amplitude of the Ca^{2+} signal. To confirm that the Ca^{2+} signals are responsible for the previously observed increases in mEPSPs, I have developed an analysis technique to match the Ca^{2+} signals and mEPSPs produced by the same vesicle of neurotransmitter. This approach matches the two events correctly. Our data suggests that in most cases, there is a correlation between Ca^{2+} signal amplitudes and mEPSP amplitudes in unstimulated preparations. This will allow us to use GCaMP imaging to study postsynaptic potentiation at these synapses. We also found no correlation in unstimulated preparations that would suggest a possible function of the muscle subsynaptic reticulum in filtering synaptic current.

Keywords: *Drosophila melanogaster, Subsynaptic reticulum, GCaMP, Miniature excitatory post-synaptic potentials, Synaptic current*

Acknowledgements

I would like to my family and friends for supporting me through my academic career. They have always encouraged me to work through the challenges and never give up.

I would also like to extend my sincere thanks to Dr. Zuloaga for agreeing to be the second reader of my thesis, providing insightful suggestions, advice, and words of support.

Lastly, I would like to express my deepest appreciation to Dr. Lnenicka for his invaluable contribution to my understanding of Electrophysiology. Without his guidance and continued support, this thesis would not have been possible. I admire his love for Electrophysiology which has been very contagious. I also cannot thank him enough for being a great mentor.

List of Figures

List of Tables

Table of Contents

Introduction

Synaptic transmission in neuronal networks are the fundamental mechanism by which neurons communicate. This process is facilitated by synaptic connections between a presynaptic neuron which secretes neurotransmitter onto a postsynaptic neuron. The postsynaptic membrane expresses neurotransmitter receptors that inhibit or excite the postsynaptic cell. The discovery of neurotransmitters has played a fundamental role in shaping theories about brain function and has helped researcher further understand the nature of synaptic transmission. Neurotransmitter molecules, also known as the chemical messenger, are discretely packaged into synaptic vesicles, and released as quantal packets into the presynaptic terminal. This phenomenon was first discovered by J. Del Castilla and B. Katz who devised the quantal hypothesis in 1954 (Del Castillo & Katz, 1954). This postulate proposed that the excitatory postsynaptic potentials (EPSP) have amplitudes that fluctuate in steps which are equal in size to miniature excitatory postsynaptic potentials (mEPSPs) and also suggested that transmitter release occurs in quantal packet that are equivalent to mEPSPs (Del Castillo & Katz, 1954). This phenomenon of mEPSPs was discovered two years before the quantal hypothesis was devised, after experiments on the frog NMJs were done by Fatt and Katz in 1952 (Fatt & Katz, 1952). They discovered that the post synaptic membrane potential recordings in the absence of nerve stimulation showed spontaneous neurotransmitter release which appeared as mEPSPs.

The earliest studies of electrophysiology are credited to Luigi Galvani, a pioneer who demonstrated the electrical basis of nervous system function. Galvani discovered electrical excitation in a frog neuromuscular preparation, using an electrostatic generator and Leyden Jar in the mid-1700s. For the past seventy years, intracellular recordings have been the predominant method for studying synaptic physiology. The use of microelectrodes or patch electrodes launched

the beginning of single cell electrophysiology. Sharp thin-tipped intracellular glass microelectrodes were first co-developed by Gilbert Ning Ling and Ralph Gerard in the 1940s to stimulate individual cells electrically and study electrical potentials (Gerard & Ling, 1949). Improvements of the microelectrode were developed by Erwin Neher and Bert Sakmann in the late 1970s. They introduced the patch clamp electrode which made it possible to record single ionic channel activity (Neher & Sakmann, 1976). Modern research has promoted the use of imaging techniques in neurophysiology. The advantage of such advancements are that they allow simultaneous monitoring of multiple cells. In addition, these techniques are less invasive, enabling cells to maintain constant membrane potentials.

Given the extensive role of Ca^{2+} in signal transduction, the discovery of fluorescent Ca^{2+} indicators has revolutionized the extent at which we are able to visualize concentrations of Ca^{2+} at a cellular level. The resting intracellular Ca^{2+} signaling concentrations in neurons is about 50-100 nM during electrical activity. These levels are said to be elevated 10 to 100 times from baseline (Berridge et. al., 2000). At the *Drosophila* NMJ, postsynaptic glutamate receptor channels are known to have permeability to Ca^{2+} (Chang et al., 1994). Na^{+}, a major charge carrier that passes through glutamate receptor channels is accompanied by Ca^{2+} which modulates receptor channel activity. This Ca^{2+} concentration should, therefore, reflect synaptic currents.

In electrophysiology, Ca^{2+} indicators are now used to monitor the electrical activity as action potentials and synaptic potentials are normally accompanied by the influx of Ca^{2+}. Previous studies have performed optical quantal analysis at the dendritic spines of CA1 pyramidal neurons in rat brain slices by imaging the transient increase in Ca^{2+} (Oertner et al., 2002). Transmitter release is able to be visualized with the use of postsynaptic Ca^{2+} indicators which detects admission of Ca^{2+} into the postsynaptic membrane of *Drosophila* (Desai & Lnenicka, 2011). Therefore, use

of fluorescent Ca^{2+} sensors such as GCaMP6 enables further analysis of synaptic physiology at the NMJ. Recording spontaneous release of Ca^{2+} at the NMJ is done using fluorescence microscopy and image analysis software. Preparations are analyzed for GCaMP6 flashes along the nerve terminal, and region of interest (ROI) are manually drawn at sites where GCaMP6 flashes occur (Akbergenova et al., 2013). The light intensity of these Ca^{2+} events in ROIs along the terminal are then quantified and analyzed. GCaMP6 is widely used for Ca^{2+} imaging and includes a circularly permuted green fluorescent protein, a calcium-binding protein calmodulin and CaM-interacting M13 peptide (Chen et al., 2013). This Ca^{2+} indicator is expressed through the GAL4-UAS system, a biochemical gene expression technique used to drive expression of a particular gene of interest in *Drosophila* (Alvarado et al., 2002). These optophysiology techniques have generally been used in a qualitative manner to reveal cell activity, however, it has not been used quantitatively to determine the magnitude of activity.

The frequency of stimulation at the synapse and changing ionic concentrations within neurons have been shown to produce changes in synaptic physiology. An increase in Ca^{2+} concentration in postsynaptic neurons has also been shown to generate synaptic plasticity as well as influence transmitter release and receptor sensitivity (Desai & Lnenicka, 2011). A leading model used for studies of synaptogenesis, synaptic plasticity, and other synaptic functions is found within the embryos and larvae of *Drosophila* (Beramendi et al., 2007).

The neuromuscular junction (NMJ) of *Drosophila* contains synaptic boutons that have 40 nm clear vesicles containing glutamate, an excitatory neurotransmitter (Jan et al., 1976; Johansen et al., 1989). Type Ib boutons and the smaller Is boutons innervate the abdominals body wall muscle fibers (Lnenicka, 2020). Within the postsynaptic region of *Drosophila* is the subsynaptic reticulum (SSR), a specialized post synaptic membrane which consists of elaborate junctional

membranes, surrounding the synaptic boutons (Budnik et al., 1996). The SSR contains ionotropic glutamate receptor subunits such as GluRIIA and GluRIIB which bind glutamate transmitter (Guan et al., 1996; Qin et al., 2005). This structure shows activity dependent junctional plasticity that regulates postsynaptic translation and morphological organization (Sigrist et al., 2000).

In this study, we examine whether Ca^{2+} indicators can be used to quantitatively measure the size of synaptic potentials. To accomplish this, we analyzed recordings of mEPSPs and GCaMP6 signals at the NMJ of *D. Melanogaster* to compare the size of spontaneous postsynaptic Ca^{2+} produced by a single vesicle of neurotransmitter with the size of its associated mEPSPs recorded with intracellular electrodes. The amplitude of the synaptic current was estimated from the amplitude of the Ca^{2+} signal which was measured using GCaMP expressed in the postsynaptic membrane. The synaptic potential was measured by the electrical recording of mEPSPs. We hypothesized that post synaptic Ca^{2+} signals can be used to quantitatively measure the size of synaptic currents and resulting synaptic potentials with the application of optophysiology techniques. Since Ca^{2+} enters through the postsynaptic receptors along with Na^{+}, the amount of Ca^{2+} that enters should ultimately reflect the synaptic current. Our findings suggest that for many NMJs, there was positive correlation between the amplitude of Ca^{2+} signals and the mEPSP signals, indicating that Ca^{2+} signals can serve well as a measure for synaptic potentials. In some cases, however, the NMJs displayed weak correlational data between Ca^{2+} signals and its associated mEPSP. This was due to Ca^{2+} signals associated with small or missing mEPSPs. A possible explanation for the lack of correlation is that the SSR is filtering the synaptic currents.

Materials and Methods

A. Recording mEPSPs in Drosophila Female Larvae and Imaging of GCaMP-expressing Larvae

Experiments were performed on muscle fiber 4 in segments 3 and 4 of wandering third-instar *Drosophila* female larvae. To access the NMJs, the larvae were pinned out in a physiology chamber. Then, an incision was made through the dorsal body wall, and internal organs were removed to expose the body-wall muscles. Segmental nerves were then cut, and the brain was removed. We used HL3.1 saline (Feng et al., 2004) with 1.5 mM Ca^{2+}. All experiments were performed at room temperature (20^{o} C).

Larvae expressing myrGCaMP6s in *Drosophila* muscle fibers were generated using the UAS/Gal4 system (Akbergenova, et al., 2018). Virgin UAS-myrGCaMP6s females were crossed with male Mef2-GAL4 flies and larvae were screened for the GCaMP marker under a dissecting microscope with a fluorescent lamp. These flies were a gift from Dr. Troy Littleton from the Department of Brain and Cognitive Sciences, Massachusetts Institute of Technology, Cambridge, United States. All flies were reared in 25° C on standard Jazz Medium (Fisher Scientific Hampton, NH).

Spontaneous mEPSPs were recorded using sharp microelectrodes (10–30 MΩ filled with 3 M KCl) that were connected to Axoclamp 2A or GeneClamp 500 (Molecular Devices, Sunnyvale, CA). Data was acquired (sampling rate 10 KHz) using a Digidata 1440A digitizer (Molecular Devices) and pCLAMP 10.3 software (Molecular Devices).

The terminals of GCaMP-expressing larvae were imaged through an Olympus BH2 upright, fixed-stage microscope equipped with epifluorescence, using a water-immersion Zeiss 40x lens (NA 0.75). Image streams were captured with a high-speed CCD camera at a frame rate of 20 Hz or 50 ms exposures. Excitation of GCaMP was produced by a 75-W xenon arc lamp

filtered through a Lambda-10 Optical Filter Changer (Sutter Instruments, Novato, CA). We used a 480 nm bandpass excitation filter, a 500-nm dichroic mirror, and a high pass 515-nm emission filter (Chroma Technology, Brattleboro, VT). MetaFluor 6.1 software (Universal Imaging, Downingtown, PA) was used for image acquisition as well as analysis. Fluorescence values were measured from the regions of interests (ROIs) for each frame. The average fluorescence value per frame for each background-subtracted ROI was saved in an Excel file.

B. Measuring and Analyzing Ca^{2+} Signals and mEPSPs

All preparations were analyzed for GCaMP flashes along the nerve terminal, and region of interest (ROI) were manually drawn to include 1 or 2 synaptic boutons (Fig. 1a). The light intensity of these Ca^{2+} events presented in ROI along the terminal were quantified.

a) b)

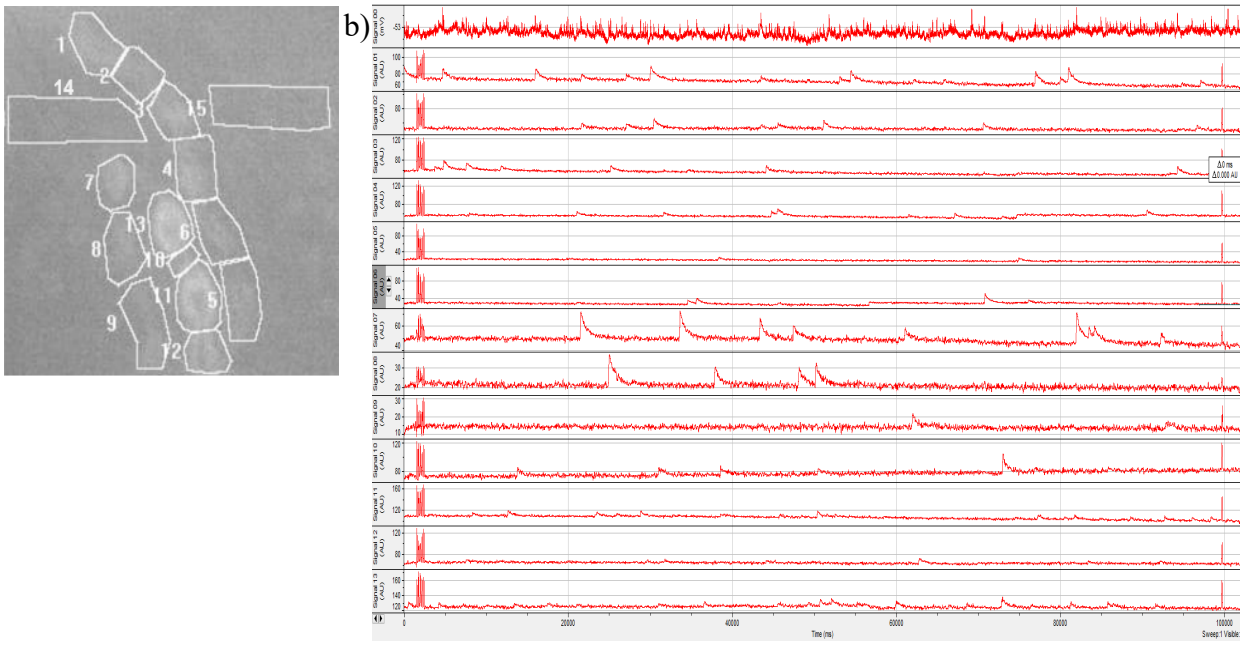

Figure 1. Synaptic boutons in the nerve terminal and Ca^{2+} signals & mEPSP recordings in Clampfit 11.2

a) Synaptic boutons in the nerve terminal were manually traced to identify ROIs. b) The corresponding Ca^{2+} signals and mEPSP recordings of this nerve terminal were quantified and presented as traces in Clampfit 11.2.

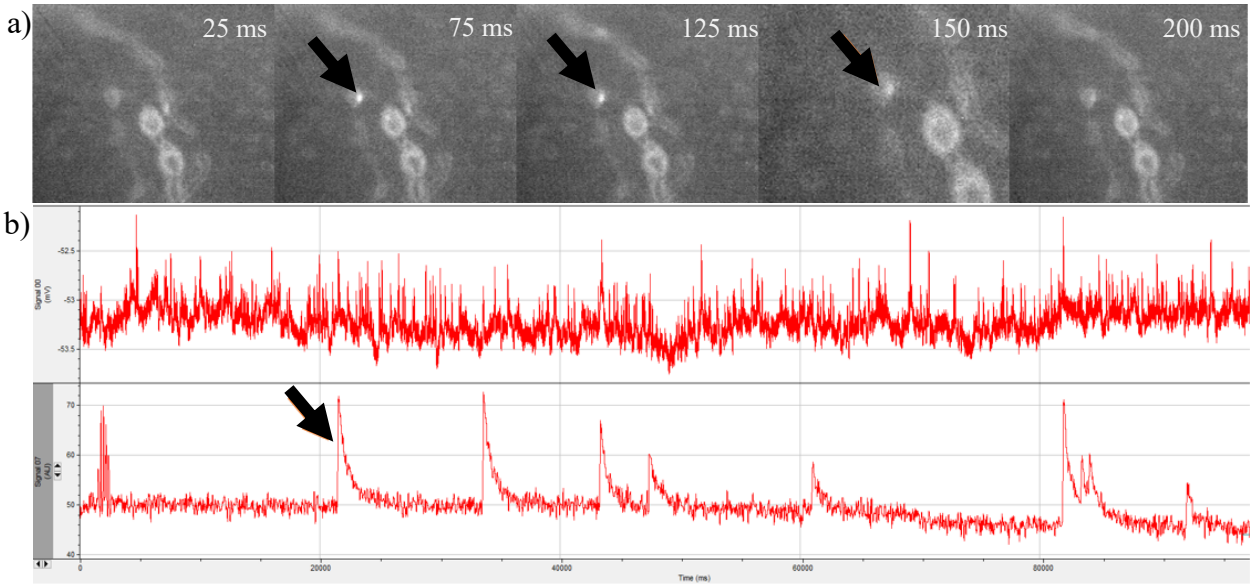

Figure 2. GCaMP flash in a synaptic bouton and Corresponding Ca^{2+} event in Clampfit 11.2. a) The red arrow points to a GCaMP flash in a synaptic bouton, indicating presence of Ca^{2+}. Each frame was taken at 50 ms exposures. b) Light intensity of the corresponding Ca^{2+} event was quantified and presented as a trace in Clampfit 11.2. The black arrow points to the corresponding Ca^{2+} event that occurred in this synaptic bouton.

Light intensity data in the form of average pixel value was converted into Clampfit traces. This was done by copying and pasting the column of average pixels values (intensity in AU) for the ROIs from SigmaPlot into Excel. These ROI values had been background subtracted in SigmaPlot. This Excel file was then saved as a Text (MS-DOS) file. This *.txt file was imported to Clampfit to display the data as traces. To do this, file/open data was opened and then the txt file was selected. The plain text converter was used with the following settings: correct number of signals were specified, units were AU, ranges were positive 1000 and negative 500, fixed-length was selected and time column was added, sampling interval was set to 50000 and start-to-start interval was set to minimum. Ca^{2+} data was subsequently displayed as traces.

The imaging system used time stamps at the beginning of the 50 ms exposures and these were adjusted so that they come at the middle of the frames and not the beginning. For example, if a single point fell within the frame, the measurement could possibly be off by up to -50ms if the

time at the beginning of the frame was used. However, if the time at the middle of the frame was used, then it could be off by ±25 ms. To make this adjustment, Ca^{2+} signals were shifted to the right by 25ms (shift time interval/right/fixed 25ms/replace wrapped samples with zeros). Finally, interpolation was used to increase the sampling rate from 20Hz to 1000Hz. This was necessary because we ultimately want to put the Ca^{2+} traces and mepsp traces in the same file and they must have the same sampling rate. This was done by using analyze/interpolation and setting the method to straight line with an Interpolation factor of 50. Data was then ready to add together with the mEPSP data after it was converted back into a text file. To do this, use Edit/Transfer traces: the Destination Window is Results window, Region to transfer is Full trace and Trace Selection should be all visible signals. The data was then ready to be transferred to the Results window where we copied and pasted it to an Excel file and save as Data.xlsx.

To prepare the mEPSP file, the abf. file was opened in Clampfit 11.2 and timing pulses in trace 2 was found. Time at the beginning of corresponding first and last timing pulses were measured. Note that the time can be directly measured at the beginning of the pulse since the sampling rate (10 KHz) is much higher than for Ca^{2+} measurements. The "delay" was then determined from the beginning of the Ca^{2+} trace timing pulse to the mEPSP trace timing pulse (mEPSP pulse – GCaMP pulse). Traces were aligned by shifting the mepsp trace to the left by the delay (shift time interval/left/fixed "delay"/replace wrapped samples with zeros). Data reduction was done such that mEPSP trace was down to 1K sampling (analyze/data reduction/method decimate/reduction factor 10). Traces were transferred as before and added to a Data xlsx. file. Channel 1 was transferred to the first column and channel 2 was transferred to the last column. The final rows of data were eliminated where there are missing values or 0s. This file was then saved as a text file and opened in Clampfit 11.2 as before. Note that the sampling interval is now

100 us (1 KHz). The Clampfit file was then saved as an abf. file (axon binary file floating point) and used for future analysis.

Ca^{2+} data and mEPSP data that populated as separate traces were placed into a Clampfit file where traces lined up, such that data recordings start at the same time. This allowed us to match Ca^{2+} signals to their corresponding mEPSPs. The Ca^{2+} data that came from MetaFluor is text data- the frame times lined up in rows with the average ROI pixel value (AU) for that exposure. Note that MetaFluor gave frame times as the time at the beginning of the exposure. MiniAnalysis was subsequently performed on the Ca^{2+} data and the mEPSP traces for statistical analysis of trace signals.

C. Synchronization of mEPSPs and Ca^{2+} signals in Clampfit 11.2 Software

To align Ca^{2+} traces with the mEPSP traces so that the times were synchronized, a timing light pulse was used. An LED was placed in the light path of the imaging system and a 50ms square voltage pulse was then sent to the LED and also to the mEPSP trace. By aligning the light pulse in the Ca^{2+} trace with the voltage pulse in the mepsp trace, the two traces were synchronized as shown in Fig. 2. Note that the way the experiment was configured caused the mEPSP trace to start slightly before the GCaMP imaging. Ideally, we wanted the 50 ms light pulse to fall exactly within a 50 ms exposure. Under such conditions, the frame time would indicate the beginning of the light pulse. To get close to this, five staggered light pulses were delivered at the beginning of imaging. The pulse from the background trace with the largest amplitude was selected and used for measurements. Since light pulses rarely fell exactly in a single frame but spanned two frames, further adjustment were made. Starting with the largest pulse and assuming the pulse spans 2 exposures, time of second frame - (50 ms x Au for first frame/total AU for 1^{st} + 2^{nd} frame) was taken. Note that the frame time would be at the peak for each frame, therefore, it should be a

multiple of 50ms. The number of the light pulse (1-5) were recorded as well as its start time. The same procedure was done to determine the time at the beginning of the final pulse. To view the 50ms timing pulses, the background values were used after subtracting the baseline values.

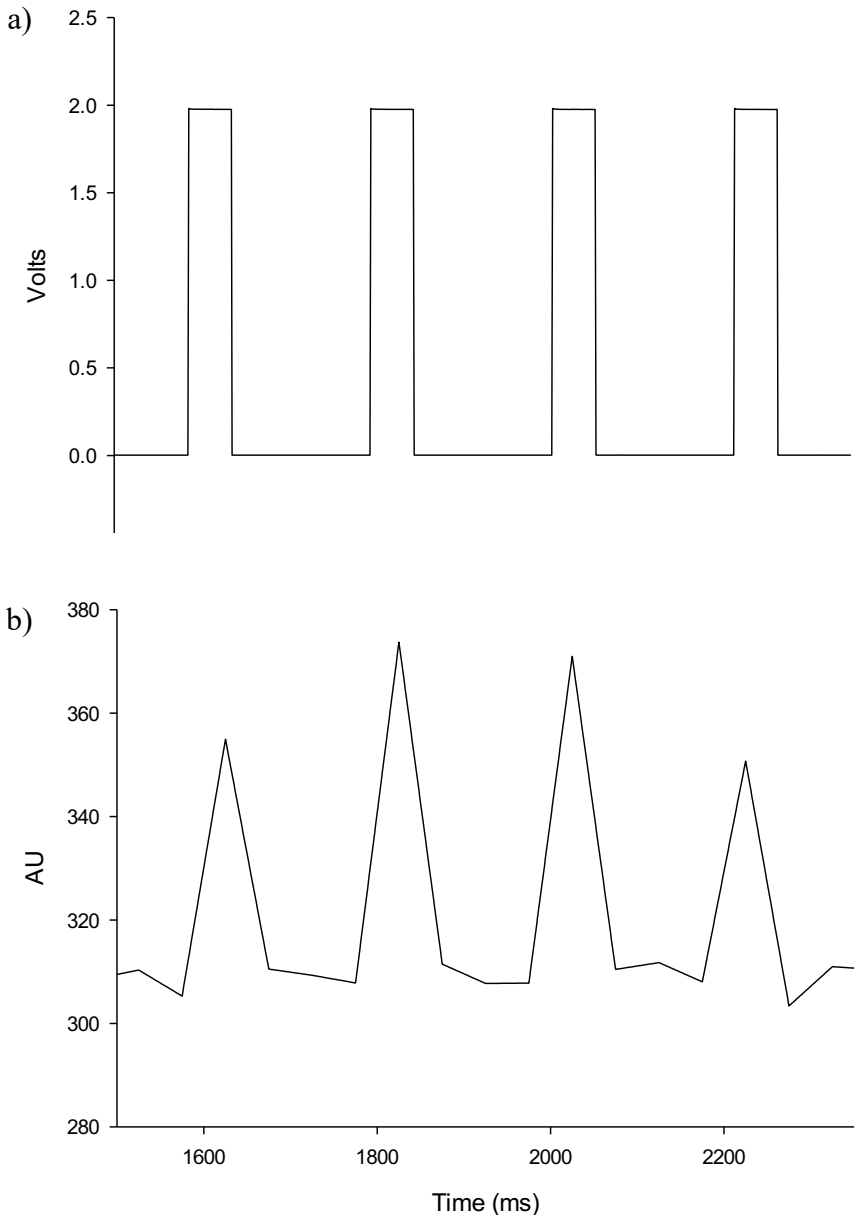

Figure 3. Voltage pulse sent to the mEPSP trace and to LED and recorded as light intensity in Ca^{2+} trace.

a) A 50ms square voltage pulse was sent to the mEPSP trace. b) An LED was placed in the light path of the imaging system and a 50 ms square voltage pulse was then sent to the LED and recorded as light intensity in the Ca^{2+} trace.

D. Statistics for Ca^{2+} signals and Corresponding Spontaneous mEPSP in Clampfit 11.2

MiniAnalysis data was used to pinpoint Ca^{2+} signals and its corresponding mEPSP in Clampfit traces. To obtain the half-time of the mEPSP signals, we used the time (ms) – Rise 50 which was pasted into the excel. The estimated time of the Ca^{2+} signal taken from MiniAnalysis and an exact time of event, was recorded using cursors in Clampfit 11.2. Cursor 1 was set to record the half-rise of the Ca^{2+} signal. Note that the half-rise of the Ca^{2+} signals were manually taken because automated analysis does not account for an prolonged peak as seen in some Ca^{2+} signals. Cursors were then appended. This data analysis was done for every Ca^{2+} signal.

E. Integration of Statistics into SigmaPlot 12.0

Cursor times and statistics were compiled and integrated using SigmaPlot 12.0 for further analysis. Using SigmaPlot 12.0, Ca^{2+} signals and corresponding mEPSPs from MiniAnalysis were placed side by side. Ca^{2+} cursor measurements were corrected for time by a factor of 1.00025 ms. Parameters such as region size (μm^2), corrected region size (μm^2), terminal type and integrated calcium signals ($Au \cdot \mu m^2$) were added for further statistical analysis. Region size was multiplied by a factor of 0.045 to convert pixels to μm^2, and the integrated calcium signal ($Au \cdot \mu m^2$) was calculated by multiplication of peak amplitude (AU) and corrected region size (μm^2). For correlational analysis, integrated calcium signals were graphed against peak mEPSP amplitudes using scatter plots and the Pearson coefficient was added to understand data correlation.

F. Identifying the mEPSP that Corresponded to the Ca^{2+} signal

To identify the mEPSP that occurred synchronously with a Ca^{2+} signal in a unbiased way, we created an automated excel spreadsheet that accurately correlate measured Ca^{2+} signals with the closest corresponding spontaneous mEPSP signal. The Excel formulas calculated the intervals from each Ca^{2+} signal to all the mEPSPs and then identified the nearest interval.

Offset	43						
					Min Absolute interval		18.0107
					Min interval Row		18.0000
					mEPSP amplitude address	C18	
					mEPSP Amplitude		0.2870
					mEPSP time address	B18	
					mEPSP time		3225.8000
					INTERVAL (GCAMP-MEPSP)		18.0107
					GCaMP time		3243.81075
mEPSP Time	Pre - Offset	mEPSP Amp					
1,355.90	1,312.90	0.861			**Intervals (absolute values)**		1,930.91
1,610.30	1,567.30	0.256					1,676.51
2,178.30	2,135.30	0.867					1,108.51
2,270.30	2,227.30	0.323					1,016.51
2,651.30	2,608.30	0.854					635.51
2,760.40	2,717.40	1.141					526.41
2,897.80	2,854.80	0.653					389.01
3,205.10	3,162.10	0.635					81.71
3,268.80	3,225.80	0.287					18.01

Figure 4. Excel spreadsheet used to calculate GCaMP signal's nearest associated mEPSP.
An Excel spreadsheet was used to calculate the GCaMP signal's nearest associated mEPSP signal. This spreadsheet compiled all signals and its corresponding data as highlighted in dark gray which provided parameters such as the mEPSP amplitude, time of signals, and interval. Note, this image only illustrates a single Ca^{2+} signal (GCaMP) and a few of the intervals to the mEPSPs.

Data from MiniAnalysis calculated the mEPSP time which was added to the Excel sheet. An offset was added to the mEPSP data to correct for time which enabled synchronization of Ca^{2+} and mEPSP traces. Corrected GcAMP half-rise times were subtracted from all mEPSP signals to obtain the nearest mEPSP signal as shown in Fig. 3. With this, we were able to obtain data that included the time difference in Ca^{2+} and mEPSP signals which were recorded in intervals, corresponding amplitudes of the mEPSP signal, and the exact time of corresponding mEPSP signals. Data analysis was further performed which gave results pertaining to the frequency at which the corrected Ca^{2+} half-time minus the corrected mEPSP half-time occurred. This data was placed in 25 ms bins that ranged from -500 to +500 ms. The data was normalized and histograms were created to display frequency of intervals regarding the difference in GCaMP half-time and mEPSP half-time. Ca^{2+} amplitude and its corresponding mEPSP amplitude were also graphed on scatter plots with corresponding r^2 and p-values.

Results

To analyze the correlation between Ca^{2+} signals and mEPSPs, the time at ½ amplitude of Ca^{2+} signals and its mEPSPs were recorded at the *Drosophila* NMJ. By doing this, we are able to compare the size of spontaneous postsynaptic Ca^{2+} signals produced by a single vesicle of neurotransmitter with the size of its associated mEPSP. We examined the intervals between postsynaptic Ca^{2+} signals and the mEPSP. As discussed in the Methods section, raw Ca^{2+} signals and mEPSP data were displayed as separate traces and aligned using an LED placed in the light path. A 50ms square voltage pulse was sent to the LED and displayed in the mEPSP trace. By aligning the light pulse in the Ca^{2+} trace with the voltage pulse in the mEPSP trace, we could synchronize the two traces (Fig. 3). The time for each Ca^{2+} signal was subtracted from all mEPSP times in an Excel spreadsheet, to determine the nearest mEPSP (Fig. 4).

A. Intervals between Ca^{2+} Signals and its Nearest mEPSP

The time interval between the Ca^{2+} signal and its nearest neighboring mEPSP was identified and intervals were graphed into 25 ms bins, ranging from -500 to 500 ms. On average, most events fell within intervals 0 to +25 ms and -25 to 0 ms. We calculated the number of expected occurrences for each of these intervals, assuming that mEPSPs occurred randomly: expected events = 0.025 s · mEPSP frequency. These values were normalized to the total number of intervals (number of Ca^{2+} signals) and expressed as a percentage. These predicted occurrences would represent the upper limit, given that in the rare cases, mEPSPs that are predicted to occur in both intervals would only be counted once. Under these conditions, we were able to calculate the percent of mEPSP events that occur by chance and compare this data to the number of Ca^{2+} events associated to mEPSP signals.

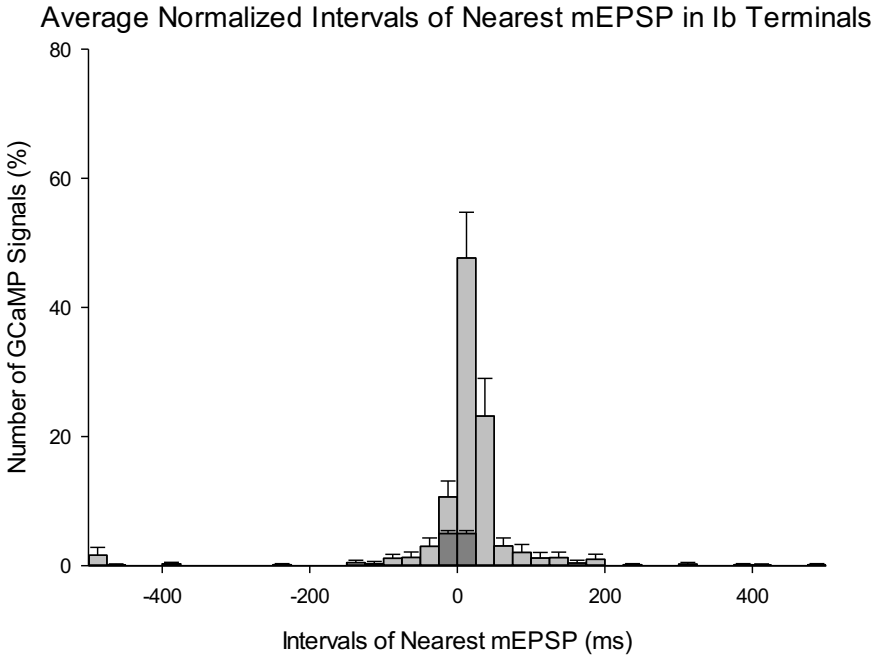

Figure 5. Nearest neighbor intervals from 9 experiments performed on Ib terminals.
The average difference in half-time of Ca^{2+} signals and half-time of mEPSP were normalized and plotted on a histogram as SEM to show the time difference of signals and the frequency at which these events occur. The average expected frequency is also plotted on the histogram from intervals 0 to +25 ms and -25 to 0 ms as SEM.

Fig. 5 displays the frequency of average normalized time intervals of the nearest mEPSPs from 9 Ib terminal preparations of the *Drosophila* NMJ. For Ib terminals, the percent of intervals seen in 0 to +25 ms (47.67 ± 7.1%) and -25 to 0 ms (10.65 ± 2.46%) were significantly greater than the expected values of "4.99 ± 0.45% standard error" ($p < .001$, *t*-test) and "4.99 ± 0.45% standard error" ($p < .05$, *t*-test), respectively. Note that experimental values for the 0 to +25 ms interval were greater than -25 to 0 ms interval. This was expected since the rate of rise for the Ca^{2+} signal was greater than that of the mEPSP. At intervals greater than ±25 ms, the expected values would decrease since many mEPSPs would occur coincidently with a mEPSP that had a shorter delay and not be counted. In the Ib terminals, it is noteworthy that time intervals less than -25 ms and greater than +50 ms demonstrated marginal signal association, indicating that the timing of

the Ca^{2+} event and its spontaneous mEPSP have resulted by chance and may simply be a result of experimental error. These overall findings suggest that an overwhelming majority of the nearest mEPSP neighbors have an associated Ca^{2+} signal within close range.

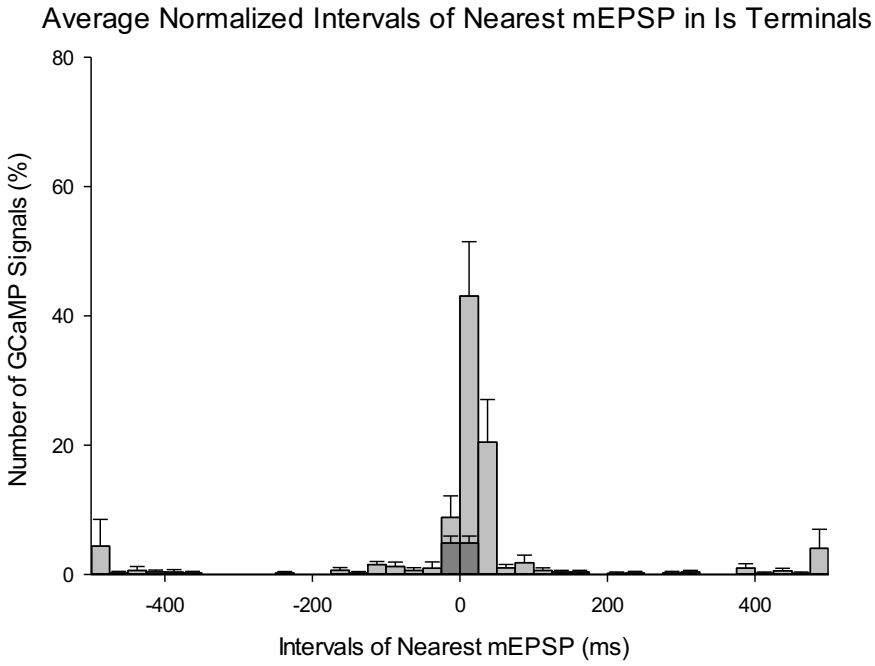

Figure 6. Nearest neighbor intervals from 8 experiments performed on Is terminals.
The average difference in half-time of Ca^{2+} signals and half-time of mEPSP were normalized and plotted on a histogram as SEM to show the time difference of signals and the frequency at which these events occur. The average expected frequency is also plotted on the histogram from intervals 0 to +25 ms and 0 to -25 ms as SEM.

Fig. 6 as shown above, illustrates the average time interval of Ca^{2+} signals and its associated mEPSP in 8 Is terminal preparations. For Is terminals, the percent of intervals seen in 0 to +25 ms (43.08 ± 8.4%) and -25 ms to 0 (8.84 ± 3.3%) were significantly greater than the expected values of "4.89 ± 1.07%" ($p < .000492$, *t*-test) and "4.89 ± 1.07%" ($p < .202$, *t*-test), respectively. Note that experimental values for the 0 to +25 ms interval were greater than -25 ms to 0 interval. At intervals greater than ±25 ms, the expected values decrease since many mEPSPs coincidently fell

within these intervals. Therefore, Ca^{2+} signals within the Is terminals associated with a mEPSP from -25 to +25 ms were not produced by chance.

B. Positive Correlation of Ca^{2+} Amplitudes and mEPSP Amplitudes

We compared the size of spontaneous postsynaptic Ca^{2+} produced by a single vesicle of neurotransmitter with the size of its associated mEPSP. This was done by measuring the amplitude of the synaptic potential and Ca^{2+} signal at the *Drosophila* NMJ. As stated in the Methods, integrated calcium signals ($Au \cdot \mu m^2$) were calculated by multiplying the peak amplitude (AU) and corrected region size (μm^2). These signals were graphed against peak mEPSP amplitudes using scatter plots and a linear regression line was fit to the data. Table 1 displays a record of all experiments done on the Ib and Is terminals in addition to statistical parameters which include r^2 values, number of events, and p-values. In general, this data revealed a positive correlation in 5 of 9 experiments seen in the Ib terminals. In the Is terminals, 5 of 8 experiments show positive correlation. Data for one of the Ib terminals is shown in Fig. 7 and 8. There is positive correlation between mEPSP amplitude and the integrated Ca^{2+} amplitude in the Ib terminal (Fig. 8). This data produced an r^2 value of .49 and a *p-value* of .00002 as seen in preparation Ib1 (Table 1). Note that this preparation was chosen for low noise levels with a data sample of 29 Ca^{2+} signals. Fig. 9a illustrates a small Ca^{2+} amplitude of roughly 10 AU paired with a small mEPSP that displays an estimated amplitude of .6 mV. These signals are notably smaller compared to the Ca^{2+} signal and mEPSP in Fig. 9b which show a large Ca^{2+} amplitude of roughly 16 AU and a large mEPSP amplitude of .8 mV. This is representative of the positive correlation of Ca^{2+} and mEPSP amplitudes shown in Fig. 8. When analyzing the nearest mEPSP and time difference from the Ca^{2+}, findings were consistent with average Ib terminal statistics where 58.62% of Ca^{2+} events fell within 0 to +25 ms of the mEPSP, significantly above chance levels. Fig. 7 shows that the number of

events exceeding the expected frequency of 4.11%, indicating that the associated signals are not random.

Table 1
Statistical Analysis of Ca^{2+} Amplitudes and Associated mEPSP Amplitudes in Ib and Is Preparations

Preparation Ib	**n**	r^2	***p-value***
Ib1	29	.49*	.00002
Ib2	54	.43*	.00001
Ib3	76	.04	.08
Ib4	65	.02	.27
Ib5	20	.35*	.006
Ib6	26	.34*	.002
Ib7	47	.01	.5
Ib8	32	.11	.065
Ib9	14	.29*	.046
Preparation Is	**n**	r^2	***p-value***
Is1	54	.19*	.0009
Is2	31	.001	.87
Is3	68	.22*	.00007
Is4	41	.46*	.00001
Is5	20	.07	.27
Is6	64	.28*	.00001
Is7	33	.05	.22
Is8	52	.17*	.0003

*p-value < *0.05*

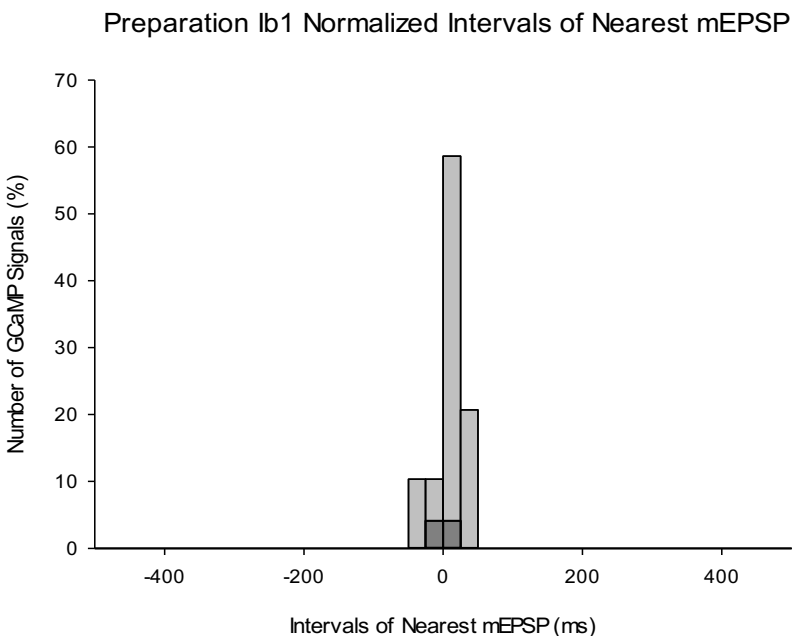

Figure 7. The nearest neighbor intervals were performed on Ib1 terminals of *Drosophila*. The difference in half-time of Ca^{2+} signals and half-time of mEPSP were plotted on a histogram to show the time difference of signals and the frequency at which these events occur. The expected frequency from intervals 0 to +25 ms and -25 to 0 ms is plotted on the histogram as vertical dark grey bars.

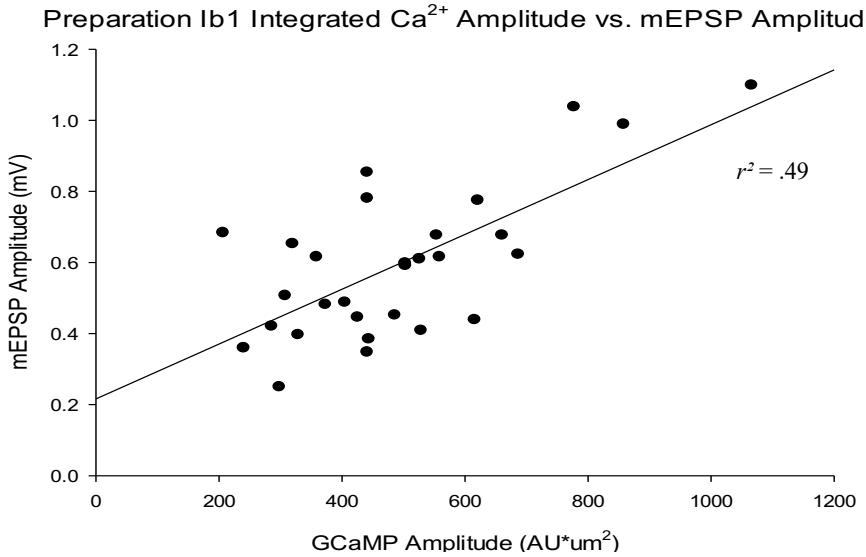

Figure 8. Ca^{2+} signal amplitude and its associated mEPSP amplitude in the Ib1 terminal. Ca^{2+} amplitudes (AU*μm²) and mEPSP amplitudes (mV) were recorded from the Ib1 terminal of Drosophila and integrated into MiniAnalysis software. 29 Ca^{2+} events were recorded and analysis was done to identify the nearest mEPSP. The amplitude of Ca^{2+} signals and its associated mEPSP amplitude was plotted on a scatter plot, as shown above.

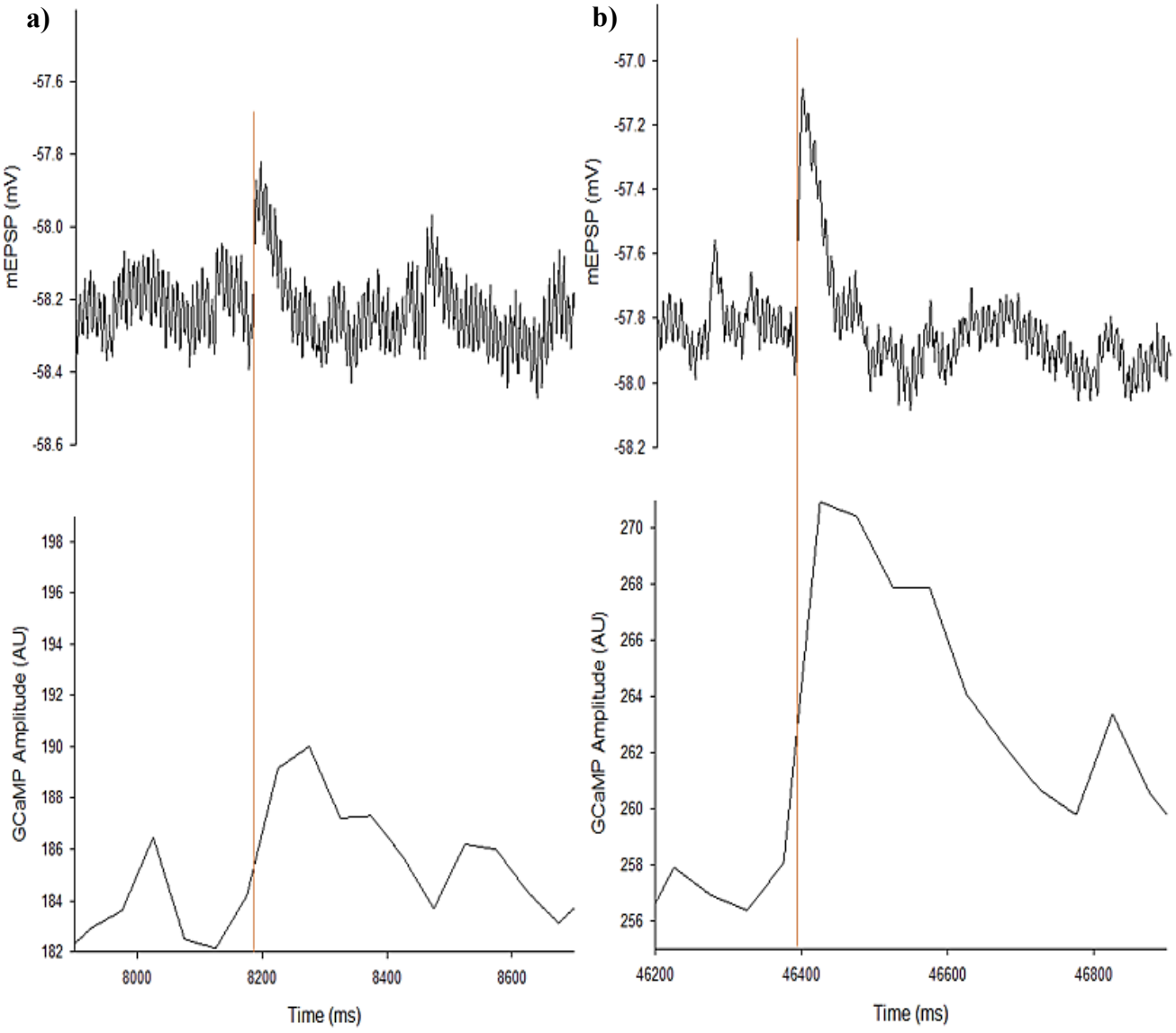

Figure 9. mEPSP and Ca^{2+} traces recorded from the Ib terminal.
mEPSP (mV) and Ca^{2+} traces (AU) were recorded from the Ib terminal and lined up in Clampfit software as shown above. a) Small Ca^{2+} amplitude is associated with a small mEPSP. b) Large Ca^{2+} amplitude associated with a large mEPSP amplitude. The red line represents the time of half-rise in both the Ca^{2+} and mEPSP trace. Graphs are appropriately scaled for comparison.

Further evidence that demonstrates the correlation between the amplitudes of Ca^{2+} signals and mEPSPs is seen for an Is terminal. Fig. 10 shows that 68.29% of all Ca^{2+} signals occur within 0 to +25 ms while 4.88% of events fell within 0 to -25 ms. The expected frequency of Ca^{2+} signals

is 3.85% of events for these intervals. There are more than expected number of events from 0 to +25 ms, indicating that these events are not random pairings. This data demonstrates that our analysis technique is able to isolate Ca^{2+} events and its associated mEPSP. Fig. 11 shows integrated calcium signals ($AU \cdot \mu m^2$) graphed against mEPSP amplitudes (mV). Once again, we notice positive correlation between the mEPSP amplitude and integrated Ca^{2+} amplitude with a r^2 of .46 and *p-value* of .00001 as seen in Preparation Is4 (Table 1). This data suggests that a large Ca^{2+} signal yields a large synaptic potential. The same is true for the latter, such that a smaller Ca^{2+} signal yields a small synaptic potential. Fig. 12a illustrates a smaller Ca^{2+} amplitude of roughly 10 AU paired with an associated small mEPSP with an estimated amplitude of .5 mV. These signals are smaller compared to associated signals in Fig. 12b which show a large Ca^{2+} amplitude of roughly 18 AU and a large mEPSP amplitude of 1.0 mV. This portrays the positive correlation of Ca^{2+} and mEPSP amplitudes demonstrated in the Is terminal. In addition, the mEPSP signal's half-rise time comes slightly before the Ca^{2+} signal half-rise time because electrical propagation which presented in the form of mEPSCs, travel faster than chemical signaling.

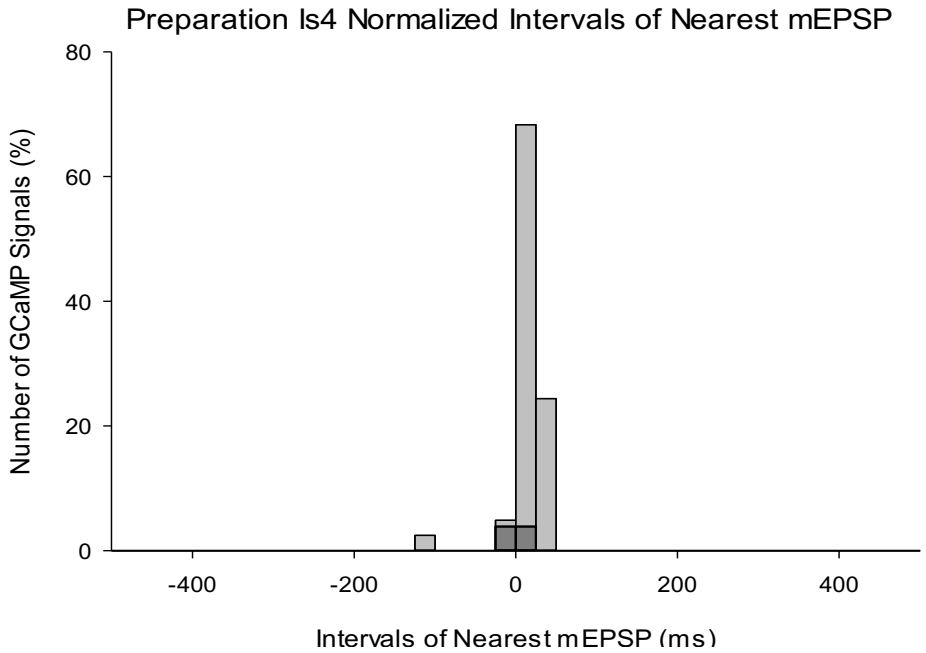

Figure 10. The nearest neighbor intervals were performed on Is4 terminals of *Drosophila*. The difference in half-time of Ca^{2+} signals and half-time of mEPSPs were plotted on a histogram to show the frequency at which these events occur. The expected frequency from intervals 0 to +25 ms and -25 to 0 ms is plotted on the histogram as vertical dark grey bars.

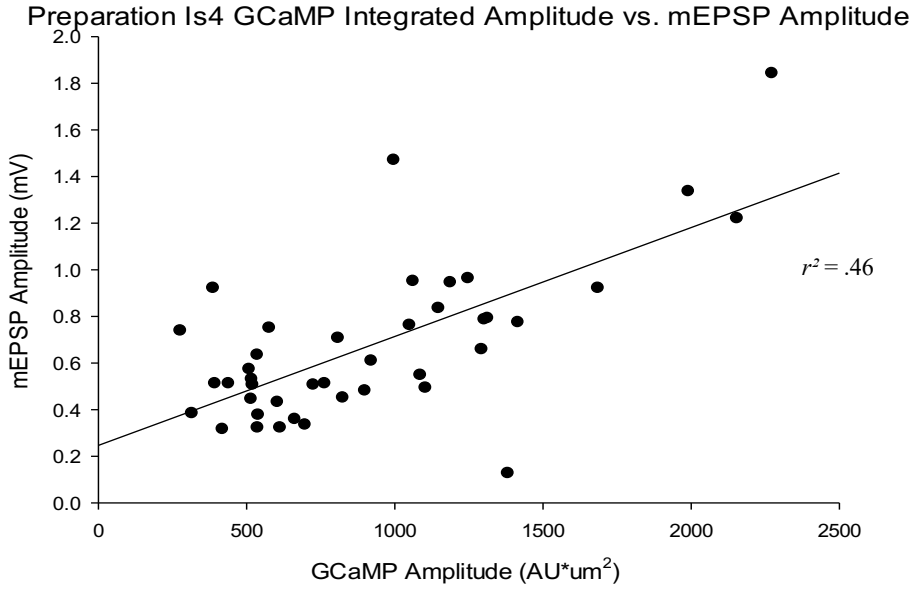

Figure 11. Ca^{2+} signal amplitude and its associated mEPSP amplitude in the Is4 terminal. Ca^{2+} amplitudes (AU*μm²) and mEPSP amplitudes (mV) were recorded from the Is4 terminal of *Drosophila* and integrated into MiniAnalysis software. 41 Ca^{2+} events were recorded and analysis was done to identify the nearest mEPSP. The amplitude of Ca^{2+} signals and its associated mEPSP amplitude was plotted on a scatter plot, as shown above.

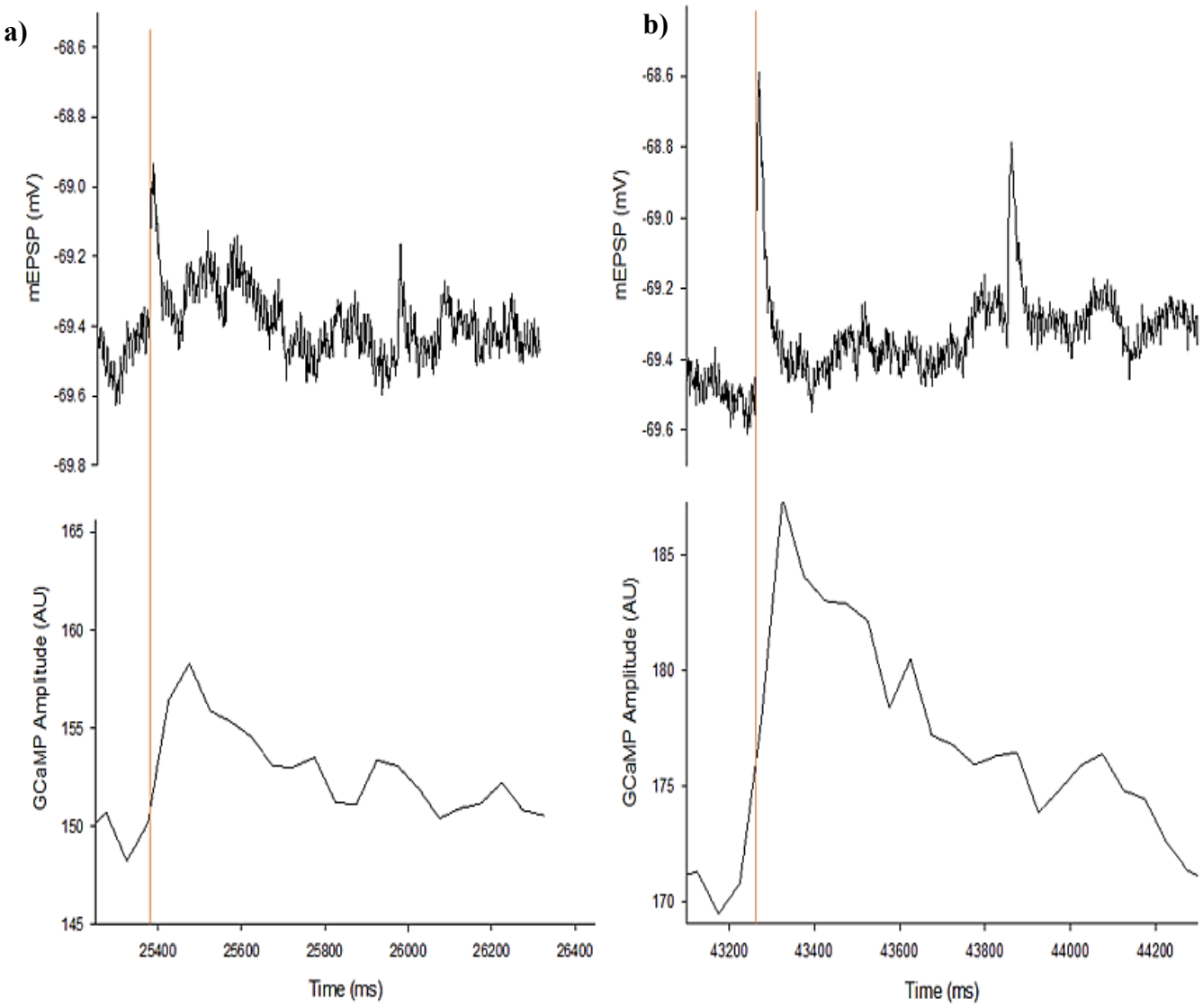

Figure 12. mEPSP and Ca^{2+} traces recorded from the Is terminal.
mEPSP (mV) and Ca^{2+} traces (AU) were recorded from the Is terminal and lined up in Clampfit software as shown above. a) Small Ca^{2+} amplitude associated small mEPSP. b) Large Ca^{2+} amplitude associated with a large mEPSP amplitude. The red line represents the time of half-rise in both the Ca^{2+} and mEPSP trace. Graphs are appropriately scaled for comparison.

C. No Correlation of Ca^{2+} Amplitudes and mEPSP Amplitudes

No correlation was observed in some preparations where the size of the mEPSP amplitude did not reflect the associated Ca^{2+} signal amplitude. These findings were shown in both the Ib and Is terminals, where preparations with low noise levels have a mEPSP which appeared to be too

large or too small, producing no size correlation with its corresponding Ca^{2+} signal. For the Ib preparation data, the time at which these events occurred are still closely related, as the percentage of events falling within 0 to +25 ms was 53.48% and the percentage of events falling within 0 to -25 ms is 27.91% of events (Fig. 13)

The sizable percent of events once again reassures us that Ca^{2+} amplitudes are more than likely matched with their respective mEPSP. The expected frequency of events in this data set was 6.47% of events in intervals 0 to +25 ms and 0 to -25 ms, which is surpassed by the number of events that fell within intervals range.

The sample size for this set of data was 47 Ca^{2+} events which yielded an r^2 of .01 and a *p-value* of .5 as displayed in experiment Ib7 (Table 1). This data suggests no correlation within the size of these events (Fig. 14). We see that some data points move far away from the simple regression line, indicating a large amplitude seen in one signal and smaller amplitude in its associated signal. Fig. 15a illustrates mEPSP and Ca^{2+} traces of raw data recorded in the Ib terminals, depicting an event where the Ca^{2+} event is notably larger than its associated synaptic potential. The mEPSP has an amplitude of roughly .4 mV and its associates Ca^{2+} signal has an amplitude of 10 AU. This event does not occur often, however a few large amplitude Ca^{2+} signals paired with a smaller synaptic current were noted. Fig. 15b illustrates the opposite event, such that Ca^{2+} signals are noted to be smaller and is associated with a large mEPSP. This example shows a mEPSP amplitude of 1.2 mV with a Ca^{2+} signal amplitude of 6 AU.

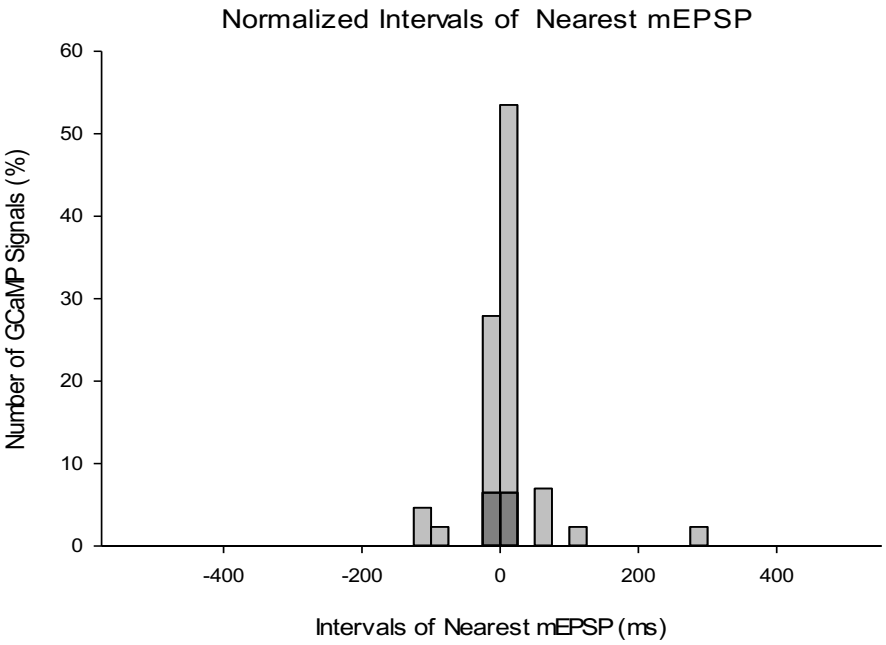

Figure 13. The nearest neighbor intervals were performed on Ib7 terminals of *Drosophila*. The difference in half-time of Ca^{2+} signals and half-time of mEPSPs were plotted on a histogram to show the frequency at which these events occur. The expected frequency from intervals 0 to +25 ms and -25 to 0 ms is plotted on the histogram as vertical dark grey bars.

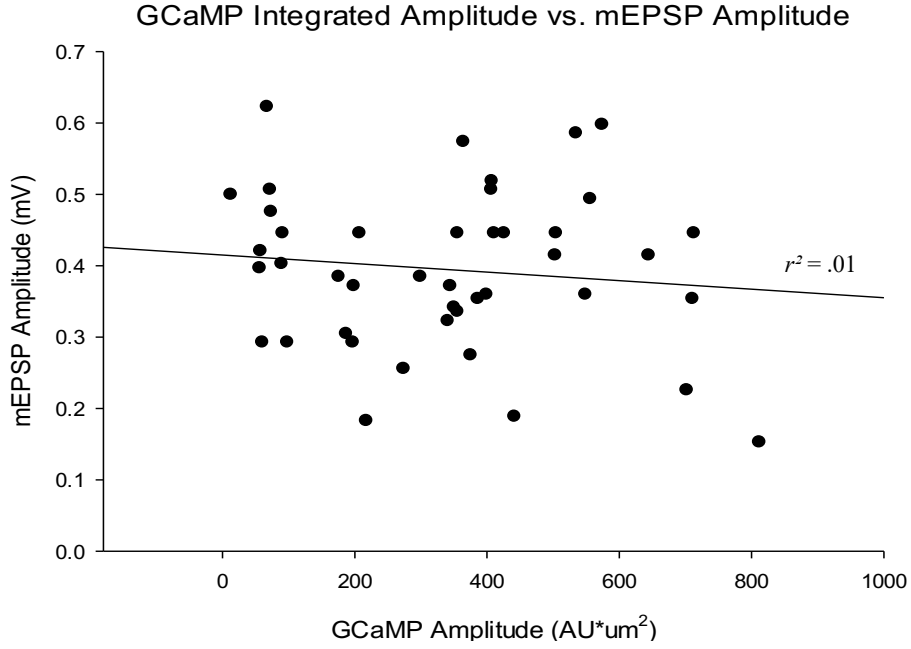

Figure 14. Ca^{2+} signal amplitude and its associated mEPSP amplitude in the Ib7 terminal. Ca^{2+} amplitudes (AU*μm²) and mEPSP amplitudes (mV) were recorded from the Ib7 terminal of *Drosophila* and integrated into MiniAnalysis software. 47 Ca^{2+} events were recorded and analysis was done to identify the nearest mEPSP. The amplitude of Ca^{2+} signals and its associated mEPSP amplitude was plotted on a scatter plot, as shown above.

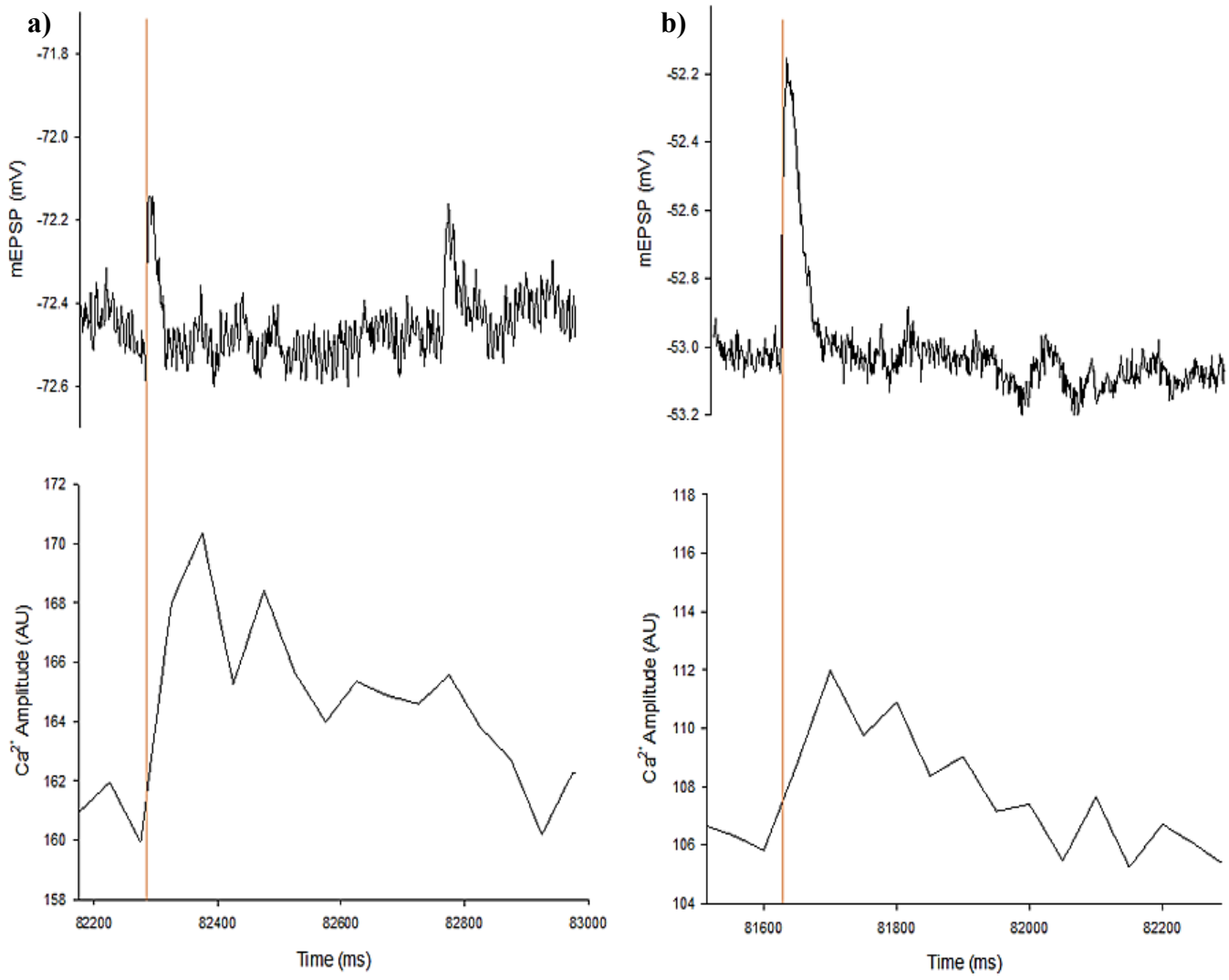

Figure 15. mEPSP and Ca^{2+} traces recorded from the Ib terminal.
mEPSP (mV) and Ca^{2+} traces (AU) were recorded from the Ib terminal and lined up in Clampfit software as shown above. a) Larger Ca^{2+} signal amplitude associated with a small mEPSP signal amplitude. Small Ca^{2+} amplitude of with an associated mEPSP with a large amplitude. The red line represents the time of half-rise in both the Ca^{2+} and mEPSP trace. Graphs are appropriately scaled for comparison.

In some cases, we also see no correlational data in the Is terminal preparation. As shown in Fig. 16, the highest frequency at which the difference in Ca^{2+} half-time and mEPSP half-time occurred was within 0 to +25 ms with 70.37% events. From +25 to +50 ms, no events fell within

this interval, and 20.37% of events fell within 0 to -25 ms. The expected frequency at which events were determined not to be random was at frequencies above 6.10% of events in intervals 0 to +25 ms and 0 to -25 ms, suggesting that over 90% of all Ca^{2+} events in this data set have true association with their corresponding signal. This evidence reassures us that signals consistently fall within ±25 seconds of eachother, indicating highly significant association of signals. Nevertheless, there is minimal correlation that exists between the Ca^{2+} amplitude and mEPSP amplitude in this preparation. As seen in experiment Is1 of Table 1, this data set included a sample size of 54 Ca^{2+} events with an r^2 value of .19 and a *p-value* of .0009. Fig. 17 indicates that some signals have amplitudes that are not similar in size when compared to their counterpart. Signals that are far from the simple regression line are characterized as either a Ca^{2+} signal with a small mEPSP, or a Ca^{2+} signal with a large mEPSP. As shown in Fig. 18a, we notice a small Ca^{2+} signal of roughly 5 AU associated with a large mEPSP signal of an estimated .9 mV. Fig. 18b shows a similar event, illustrating a small Ca^{2+} signal of 8 AU in amplitude and an associated mEPSP of 9 mV in amplitude. In very rare cases, we also observed Ca^{2+} signals that were not associated with a mEPSP which was denoted as 'missing mEPSPs' as shown in Fig. 19.

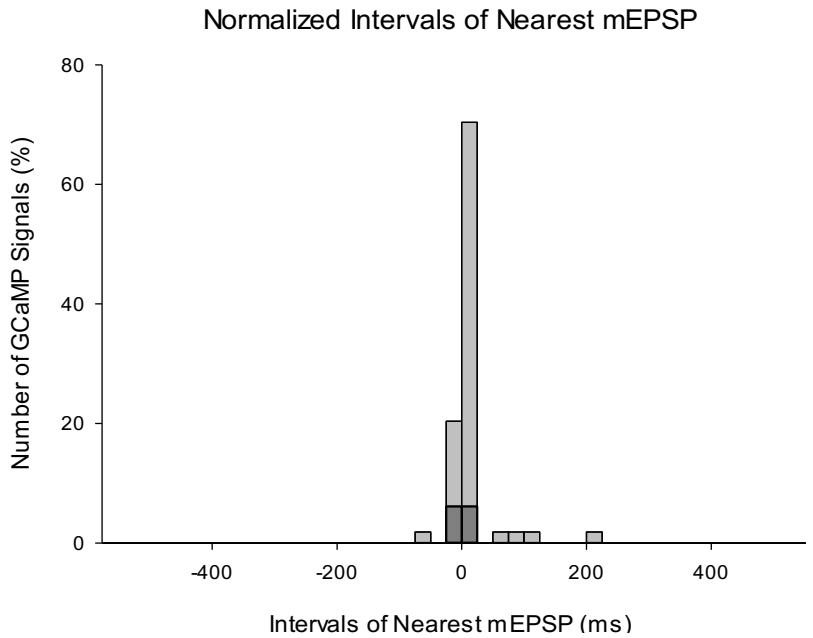

Figure 16. The nearest neighbor intervals were performed on Is1 terminals of *Drosophila*. The difference in half-time of Ca^{2+} signals and half-time of mEPSPs were plotted on a histogram to show the frequency at which these events occur. The expected frequency from intervals 0 to +25 ms and -25 to 0 ms is plotted on the histogram as vertical dark grey bars.

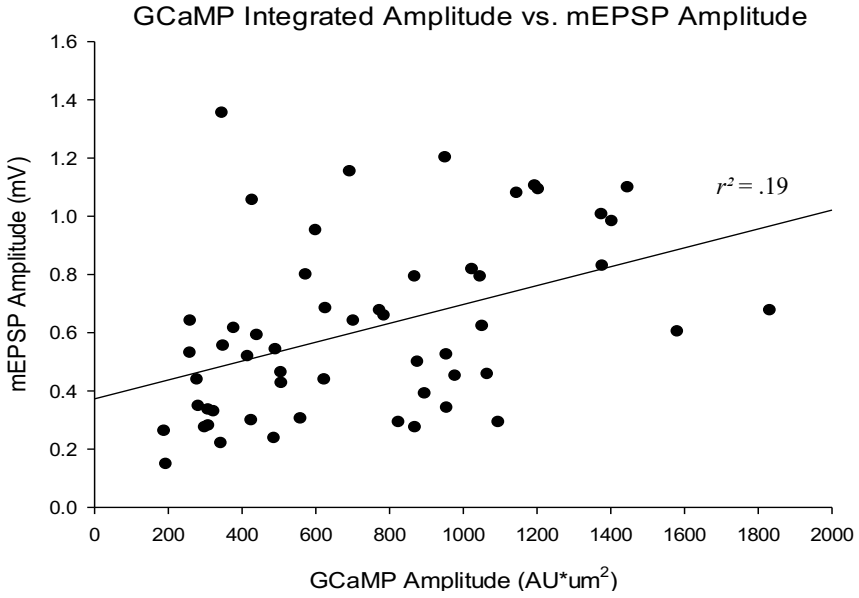

Figure 17. Ca^{2+} signal amplitude and its associated mEPSP amplitude in the Is1 terminal Ca^{2+} amplitudes (AU*μm²) and mEPSP amplitudes (mV) were recorded from the Is1 terminal of *Drosophila* and integrated into MiniAnalysis software. 54 Ca^{2+} events were recorded and analysis was done to identify the nearest mEPSP. The amplitude of Ca^{2+} signals and its associated mEPSP amplitude was plotted on a scatter plot, as shown above.

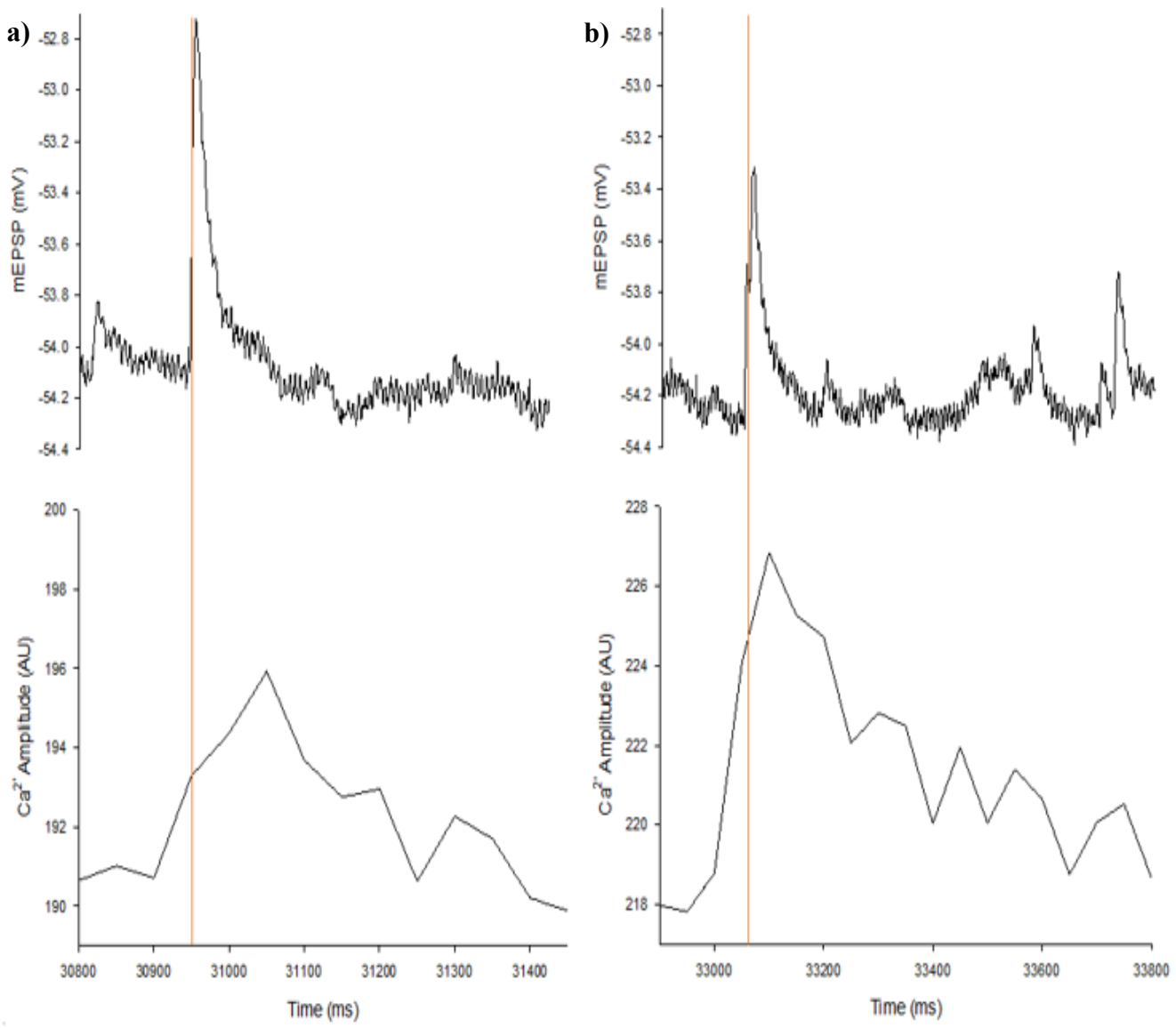

Figure 18. mEPSP and Ca^{2+} traces recorded from the Is terminal.
mEPSP (mV) and Ca^{2+} traces (AU) were recorded from the Is terminal and lined up in Clampfit software as shown above. a) Small Ca^{2+} signal associated with a large mEPSP signal. B) Small Ca^{2+} signal as well with a large mEPSP signal. The red line represents the time of half-rise in both the Ca^{2+} and mEPSP trace. Graphs are appropriately scaled for comparison.

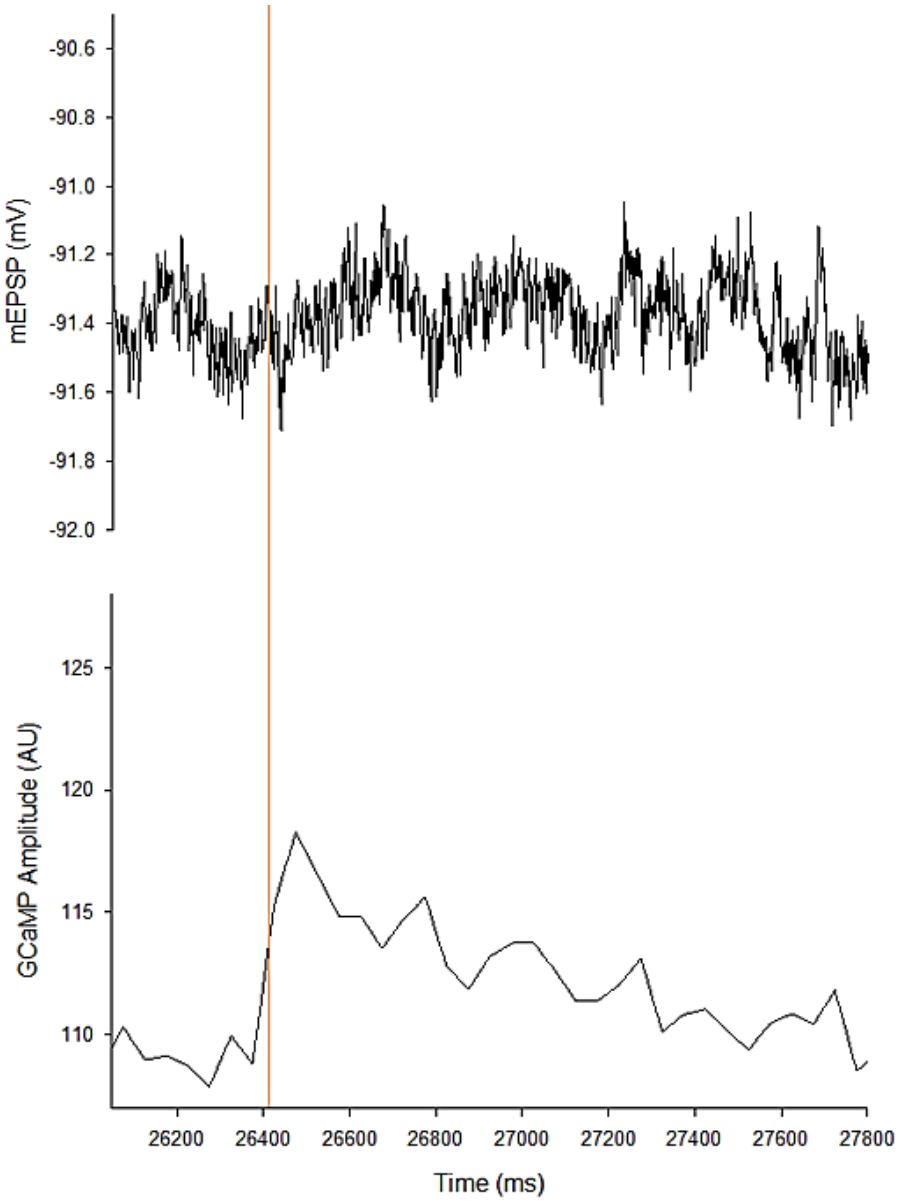

Figure. 19. mEPSP and Ca^{2+} traces recorded from the Ib terminal show rare 'missing mEPSP'. mEPSP (mV) and Ca^{2+} traces (AU) were recorded from the Is terminal and lined up in Clampfit software as shown above. These traces illustrate a Ca^{2+} signal that is not associated with a mEPSP signal, or in other words, we observe a 'missing mEPSP'.

D. Analysis of Ca^{2+} and mEPSP Amplitudes from Ib and Is Terminals of the same Muscle Fiber

In the Ib and Is terminals of the same muscle fiber, Ca^{2+} and mEPSP amplitudes were recorded and statistical analysis was performed. What we observed is that the Ib terminal will sometimes demonstrate positive correlation while an Is terminal will show no correlation, or vice versa. This finding suggests that the correlation of Ca^{2+} signals and its mEPSP amplitude are not muscle specific, but terminal specific.

In Fig. 20a, we see that the Ib8 terminal has an r^2 value of .11, indicating no correlation with a *p-value* of .065 and data sample of 32 events. On the other hand, the Is6 preparation exhibits positive correlation regarding Ca^{2+} to mEPSP amplitudes (Fig. 20b). This data set has an r^2 of .28 and a *p-value* of .00001. The Ib7 terminal shown in Fig. 20c, displays data notable for an r^2 of .01, suggesting no correlation, with a *p-value* of .05 and a data sample of 47 events. The Is3 terminal, however, shows positive correlation. We notice an r^2 value of .22 with a *p-value* of .00007 and data sample of 68 events (Fig. 20d). The opposite effect is seen, such that the Ib6 terminal yields positive correlation and the Is terminal shows no correlation. As shown in Fig. 20e, the Ib terminal has a positive correlation, bearing an r^2 value of .34 with a *p-value* of .002 and a data sample of 26 events. The Is2 terminal on the other hand, shows no correlation, yielding an r^2 of .001, *p-value* of .87 and a data sample of 31 events, as demonstrated in Fig. 20f. Refer back to Table 1 for statistics.

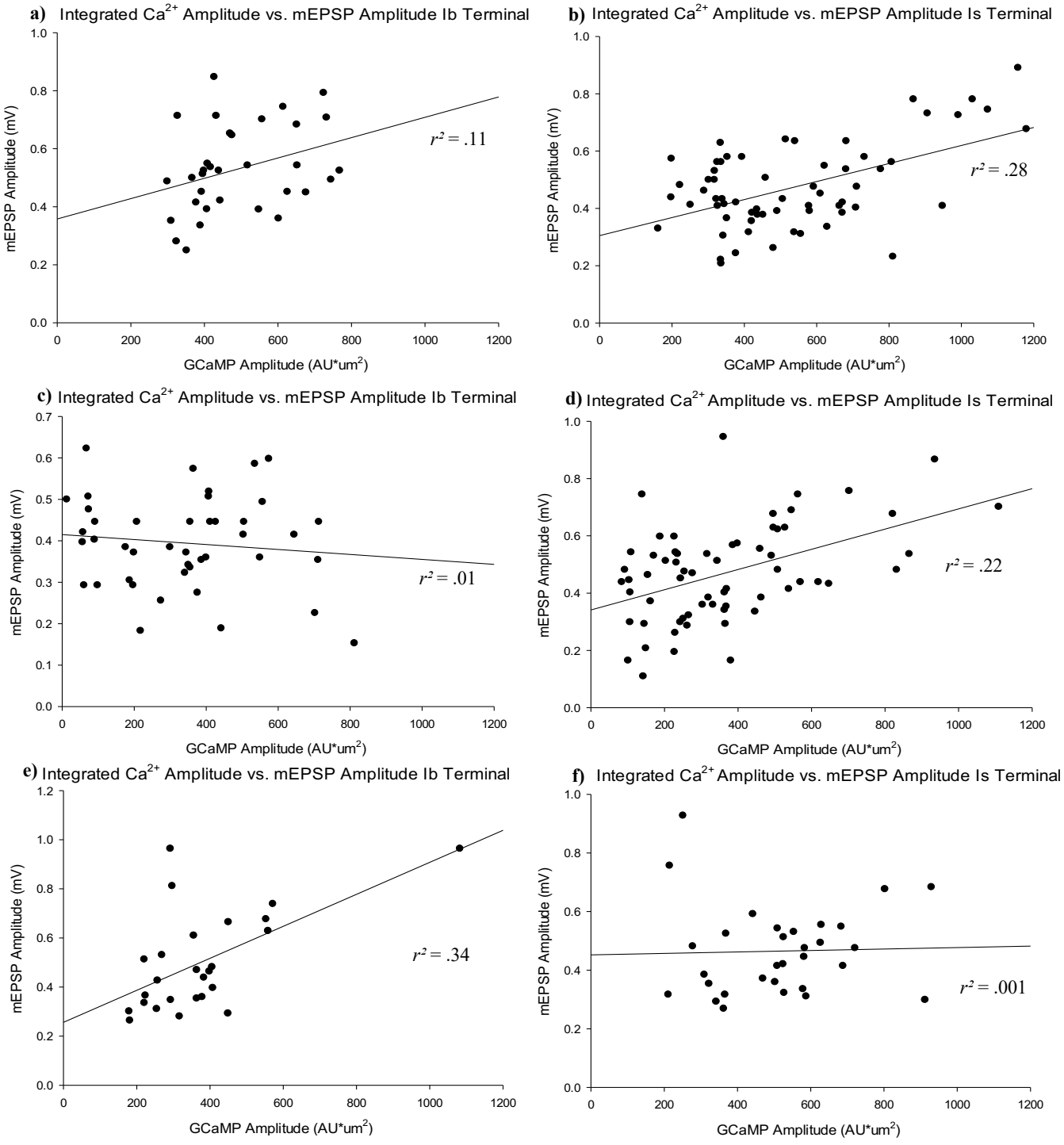

Figure 20. Ca^{2+} and associated mEPSP amplitude of Ib and Is terminal at same muscle fiber. The amplitude of Ca^{2+} signals and its associated mEPSP amplitude was plotted on a scatter plot, as shown above. A simple regression line and r^2 value was added for correlational analysis. Note that Graph A and B are from the same muscle fiber, Graph C and D are from the same muscle fiber, and Graph E and F are from the same muscle fiber.

Discussion

The advent of genetically encoded Ca^{2+} indicators and optogenetics have revolutionized event detection within biological systems. Widespread application of this technology has made headway into the field of neuroscience. Given the ubiquitous role of Ca^{2+} in signal transduction, fluorescent Ca^{2+} indicators has enabled visualization of real-time *in vivo* Ca^{2+} concentrations at the cellular level. In electrophysiology, standard technique utilizes Ca^{2+} indicators to monitor electrical synaptic activity as action potentials and synaptic potentials are accompanied by the influx of Ca^{2+}. Such advancements have provided a way to monitor neural activity in a highly specific and non-invasive way.

In this study, we examined whether Ca^{2+} indicator can be used as a quantitative means to measure the size of synaptic potentials. We hypothesized that post synaptic Ca^{2+} signals can be used to quantitatively measure the size of synaptic potentials with the application of optophysiology techniques. Since Ca^{2+} enters through the postsynaptic receptors along with Na^{+}, the amount of Ca^{2+} that enters should ultimately reflect the synaptic current. mEPSPs and Ca^{2+} signals were recorded at the NMJ of *D. Melanogaster* and statistical analysis was performed. To determine if there was correlation between Ca^{2+} signals and mEPSP, we first developed an analysis technique to determine the closest mEPSP of a given Ca^{2+} signal and the expected frequency of mEPSPs within 0 to +25 and 0 to -25 ms of a Ca^{2+} signal. We then analyzed the amplitudes of Ca^{2+} signals and its neighboring mEPSP to understand their size correlation.

Using our analysis technique, we found that the time between the Ca^{2+} signals and mEPSP events in the Is and Ib terminals largely fell within time intervals of 0 to +25 ms and 0 to -25 ms. The percent of events that within these intervals were significantly above levels of chance. We

observed most mEPSPs fell within 0 to +25 ms of its associated Ca^{2+} signal. These findings are in line with existing literature of chemical and electrical signal propagation within cells.

We wanted to know if Ca^{2+} indicators can quantitatively measure the size of synaptic potentials. Our findings suggest that while most Ca^{2+} and mEPSP signals show a positive correlation in amplitude, a few experiments demonstrated no correlation. In some preparations, we find strong positive correlation while other preparations display no correlation. Within Ib terminal experiments, we observed 5 out 9 experiments with positive correlational data (Table 1). On the other hand, in the Is terminal experiments we saw 5/8 experiments with positive correlation. This data suggests that the amplitude of the postsynaptic Ca^{2+} signal reflects the amplitude of the synaptic potential with which it is associated (Fig. 9, Fig. 12). On the other hand, we find that some preparations have no correlation. These results are likely due to the absence of correlation in Ca^{2+} and mEPSP amplitude. When looking at raw data traces, we noticed that some Ca^{2+} signals were notable for their small amplitude and a large corresponding mEPSP signal, while other Ca^{2+} signals had a larger amplitude corresponding with a mEPSP amplitude (Fig. 15, Fig. 18).

Recordings of GCaMP and mEPSP amplitudes in the Ib and Is terminals of the same muscle fiber were done for comparative analysis. What we observed is that within a given muscle fiber, the Ib terminal can exhibit positive correlational data regarding Ca^{2+} amplitude and mEPSP while the Is terminal, can demonstrate no correlation within its data set and vice versa. These findings suggest that that the correlation of Ca^{2+} and mEPSP amplitudes are not specific to the terminal.

The lack of correlation that we observe can be attributed to a variability in size of the intracellular Ca^{2+} signal and its pairing with an evoked mEPSPs in the postsynaptic membrane. A Ca^{2+} signal that does not reflect the synaptic current could possibly be due to variability in how

much Ca^{2+} enters through glutamate receptors which is unlikely. Another possibility would be variability of Ca^{2+} buffering along the terminal which results in a variable Ca^{2+} signals, however this also seems implausible because Ca^{2+} buffer should be evenly distributed throughout the muscle. An alternative explanation for weak correlation which plays on the variability of mEPSP signal is that the SSR is filtering current. Researchers at the University of Toronto, Christina T. Nguyen and Bryan A. Stewart published a study proposing that electronic decay within the postsynaptic structure contributed to "missing quanta" (Nguyen & Stewart, 2016). Their investigation in the role of the SSR was done by identifying spontaneously occurring synaptic events from intracellular and extracellular recordings of the Type 1b and Type 1s synaptic boutons in *Drosophila.* Their findings suggest that the frequency at which missing quanta arise is correlated with the SSR and the origin of the missing quanta is said to be a result of electronic decay of synaptic potentials along the SSR that causes failure to induce membrane voltage changes (Nguyen & Stewart, 2016). They also found that 5-10% of observed extracellular synaptic events that fail to cause a corresponding change in membrane voltage (Nguyen & Stewart, 2016).

Figure 21. Electron micrograph of the Subsynaptic Reticulum

Given that some of the Ib and Is terminals exhibited positive correlation and others showed no correlation, there is a possibility that shunting of the synaptic currents by the SSR may be influenced by previous synaptic activity. It has previously been shown that synaptic activity activates Ca^{2+}-dependent K^+ channels, which if found in the SSR, could shunt the synaptic current (Gertner et al., 2014). This would result in less synaptic current reaching the muscle fiber, causing

a smaller mEPSP. Another way the SSR can possibly influence subsynaptic currents is through contraction, such that the SSR condenses, causing ion channels to narrow which in effect, increases the resistance to current flow. This explanation would explain the occurrence of smaller mEPSPs. Future studies into this side of electrophysiology would definitely include analyzing Ca^{2+} signals and mEPSPs of stimulated at the *Drosophila* NMJ. With this, we can analyze the difference between pre-stimulation and post-stimulation experiments.

References

Beramendi, A., Peron, S., Casanova, G., Reggiani, C., & Cantera, R. (2007). Neuromuscular junction in abdominal muscles of Drosophila melanogaster during adulthood and aging. *Journal of Comparative Neurology, 501*(4), 498-508. http://doi.org/10.1002/cne.21253

Berridge, M., Lipp, P., & Bootman, M. The versatility and universality of calcium signaling. (2000). *Nature Reviews Molecular Cell Biology, 1*, 11-21. https://doi.org/10.1038/35036035

Budnik, V., Koh, Y-H., Guan, B., Hartmann, B., Hough, C., Woods, Daniel., & Gorczyca, M. (1996). Regulation of synapse structure and function by the *Drosophila* tumor suppressor gene dlg. *Neuron, 17*(4), 627-640. https://doi.org/10.1016/S0896-6273(00)80196-8

Chen, TW., Wardill, T., & Sun, Y. (2013). Ultrasensitive fluorescent proteins for imaging neuronal activity. *Nature*, *499*, 295–300. https://doi.org/10.1038/nature12354

Chang, H., Ciani, S., & Kidokoro, Y. (1994) Ion permeation properties of the glutamate receptor channel in cultured embryonic Drosophila myotubes. *The Journal of Physiology*, *476*(1), 1-16.

Del Castillo, J., & Katz, B. (1954). Quantal components of the end-plate potential. *The Journal of Physiology*, *124*(3), 560-573. https://doi.org/10.1113/jphysiol.1954.sp005129

Desai, A. S., & Lnenicka, G. A. (2011). Characterization of postsynaptic Ca2+ signals at the *Drosophila* larva NMJ. *Journal of Neurophysiology, 106*(2), 710-721. https://doi.org/10.1152/jn.00045.2011

Fatt, P., & Katz, B. (1952). Spontaneous subthreshold activity at motor nerve endings. *The Journal of Physiology*, *117*(1), 109-128.

Feng, Y., Ueda, A., & Wu, CF. (2004). A modified minimal hemolymph-like solution, HL3.1, for physiological recordings at the neuromuscular junctions of normal and mutant Drosophila larvae. *Journal of Neurogenetics, 18*(2), 377-402. https://doi.org/10.1080/01677060490894522

Gertner, M., Desai, S., & Lnenicka G. (2014). Synaptic excitation is regulated by the postsynaptic dSK channel at the Drosophila larval NMJ. *Journal of Neurophysiology*, *111*(12), 2533-2543. https://doi.org/10.1152/jn.00903.2013

Guan, B., Hartmann, B., Kho, Y., Gorczyca, M., & Budnik, V. (1996). The Drosophila tumor suppressor gene, dlg, is involved in structural plasticity at a glutamatergic synapse. *Current Biology, 6*(6), 695-706. https://doi.org/10.1016/S0960-9822(09)00451-5

Jan, L. Y., & Jan, Y. N. (1976). L-glutamate as an excitatory transmitter at the *Drosophila* larval neuromuscular junction. *The Journal of Physiology, 262*, 215–236. https://doi.org/10.1113/jphysiol.1976.sp011593

Johansen, J., Halpern, M. E., Johansen, K. M., & Keshishian, H. (1989). Stereotypic morphology of glutamatergic synapses on identified muscle cells of *Drosophila* larvae. *Journal of Neuroscience, 9*(2), 710–725. https://doi.org/10.1523/jneurosci.09-02-00710.1989

Lnenicka, G. A. (2020). Crayfish and Drosophila NMJs. *Neuroscience Letters,* 732. https://doi.org/10.1016/j.neulet.2020.135110

Nguyen, C. T., & Stewart, B. S. (2016). The influence of postsynaptic structure on missing quanta at the Drosophila neuromuscular junction. *BMC Neuroscience, 17*(1), 53. https://doi.org/10.1186/s12868-016-0290-7

Oertner, T. G., Sabatini, B. L., Nimchinsky, E. A., & Svoboda, K. (2002). Facilitation at single synapses probed with optical quantal analysis. *Nature Neuroscience*, *5*(7), 657–664. https://doi.org/10.1038/nn867

Qin, G., Schwarz, T., Kittel, R. J., Schmid, A., Rasse, T. M., Kappei, D., Ponimaskin, E., Heckmann, M., & Sigrist, S. J. (2005). Four different subunits are essential for expressing the synaptic glutamate receptor at neuromuscular junctions of Drosophila. *The Journal of Neuroscience, 25(*12), 3209–3218. https://doi.org/10.1523/jneurosci.4194-04.2005

Sauvola, C. W., Akbergenova, Y., Cunningham, K. L., Aponte-Santiago, N. A., & Littleton, J. T. (2021). The decoy SNARE Tomosyn sets tonic versus phasic release properties and is required for homeostatic synaptic plasticity. *Elife*, *10.* https://doi.org/10.7554/eLife.72841

Sigrist, S., Thiel, P., Reiff, D., Lachance, P., Lasko, P., & Schuster, C. (2000). Postsynaptic translation affects the efficacy and morphology of neuromuscular junctions. *Nature*, *405*, 1062–1065. https://doi.org/10.1038/35016598